7-8-2015

The Quantum Efficiency of CdSe Semiconducting Nanocrystals

Charles Bledsoe
Bellarmine University, charliebledsoe94@gmail.com

The Quantum Efficiency of CdSe Semiconducting Nanocrystals

Charles Bledsoe

Dr. Holt

Bellarmine University

August 18, 2015—April 20, 2016

Abstract

CdSe molecules are semiconducting nanocrystals that absorb visible light and emit broad wavelengths of light in response. They utilize electromagnetic radiation not only for emitting broad wavelengths of visible light, but for fluorescence, conducting electricity, and vibrational relaxation. The Thermal Lensing technique (TL) can be used to study the lifetimes of the excited state transitions and the various nonradiative processes molecules can undergo in order to better understand the excited state dynamics of semiconducting nanocrystals, and in turn, better understand how these molecules may be applied in solar cells, lasers, and fluorescence labeling. Using known methods, four samples of CdSe semiconducting nanocrystals were synthesized and colloidally suspended in a solution of octadecene. Their UV-Visible absorption spectra were obtained to determine the maximum visible absorption of each sample. The radii of the nanocrystals were calculated from the UV-Visible data, and then TL spectroscopy was performed to determine the lifetime of the excited states (τ). The fluorescence quantum efficiency (η), and fraction thermal load (φ) were meant to be determined, but due to limited data, were not determined successfully.

Introduction

CdSe Quantum Dots

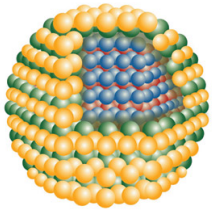

Figure 1: An artistic rendering of a QD illustrating how the atoms cluster to form the nanocrystal complex. The red and blue spheres represent the Cd and Se atoms, while the green and yellow spheres show how other atoms could envelop the core and add to the complexity of the QD.

CdSe semiconducting nanocrystals, otherwise known as quantum dots (QD), are materials of particular interest for their quantum mechanical properties.[1] The quantum properties of QD make them photoluminescent, fluorescent, and semiconducting. Another notable property of QD is the dependency of their photoluminescence on particle size, and potentially, the dependence of other properties on particle size. The size of these particles can be adjusted during the colloidal synthesis by changing the reaction time—the longer the reaction time, the larger the particles. As the size of the particles increase, so do the wavelengths of both the absorbed and emitted light. This shifting to longer wavelengths makes the particles appear redder in color, often ranging from yellow to dark red as the size increases.

Because these particles are chromophores (something that absorbs energy and emits visible light), and their photoluminescent properties are size-dependent, they can be tuned to specific sizes in order to convert visible light into specific wavelengths. This means QD can change electromagnetic energy not only into electrical energy, on account of their semiconducting properties, but can filter or absorb a broad spectrum of solar energy, depending on the particle size, and use it in a number of ways. QD use this energy in radiative processes, like fluorescence, or nonradiative processes, like vibrational relaxation, which results in the dispensing of heat energy. There may be other processes these particles undergo, marking a secondary aim of the latter analysis of the synthesized QD.

Due to these interesting properties, QD have various potentially useful applications. They can be used in fluorescence labeling due to their fluorescent properties. Once marked, a system containing QD could be screened with UV light to identify the location of the label, making it potentially useful in studying biological systems by finding how a labeled molecule is being used or where it is going. QD could also be used in solar cells. Since QD selectively absorb and emit visible and UV light, the molecules can be made in varying sizes in order to create a cell that uses different sized QD in tandem with one another to absorb a large amount of sunlight. Also due to the visible emission of these molecules, they have been considered for use in color televisions to provide clarity of color. For this same reason, they can be used in lasers; with precise synthesis and a significant energy source, they can be used to select and emit a specific wavelength of laser light. Lastly, they can be used in photodiodes since they act as semiconductors. Because they are semiconductors, when light reaches them, an electron can be promoted from the valence band into the conduction band, surpassing the band gap between the two and resulting in a flow of electricity.

Having all of these interesting properties, it is no wonder QD have been a topic of interest to many researchers. In a world with a growing energy demand coupled with a depletion of traditional fuel sources, alternative, clean sources of energy are growing ever more popular. The use of QD in newer, more energy efficient solar cells is perhaps one of their more interesting applications. If the quantum efficiency of these molecules can be optimized to give an ideal output of electrical energy, another step can be taken towards overhauling the world's energy infrastructure towards a greener, more sustainable system. Along the way towards this goal, to make these molecules even more viable for future use, they can be used in the myriad but

potentially useful applications previously mentioned—all the while learning more about them and improving their quantum efficiency.

That is the overall aim of this work. In general, a technique to effectively synthesize a varied range of QD samples and then analyze them to determine their quantum efficiency, the excited state processes they undergo, and the lifetime of those processes will be devised and utilized. The more known about how QD use excess energy, the more effectively they can be tested and then applied for use in the near future.

Excited Energy States

When excited by a significant amount of electromagnetic energy, molecules enter an excited energy state; this state is relatively short lived and the energy is rapidly dispensed through a number of excited state processes. The addition of this energy can instigate a reaction, resulting in all kinds of photochemistry depending on the system in question. If a reaction does not occur in the excited state, then there are a number of physical pathways by which a molecule can dispense excess energy. In simple molecular systems, the physical processes a molecule can undergo are either radiative or nonradiative.

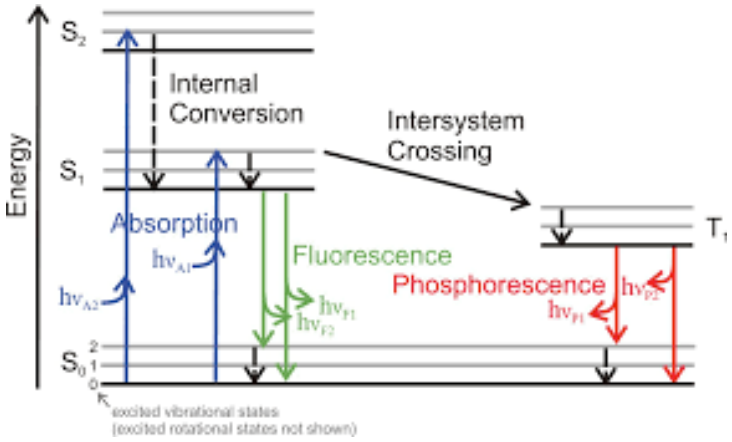

Figure 2: An example of a Jablonski Diagram displaying the various excited state processes.

Delineated by a Jablonski Diagram, as shown in Figure 2, the nonradiative processes include vibrational relaxation, intersystem crossing, and internal conversion while the radiative

processes include phosphorescence and fluorescence.[2] Vibrational relaxation is the dispensing of heat energy from the molecule by vibrations and molecular collisions; this process is a common energy shedding method in excited systems. Intersystem crossing occurs when an excited electron's spin is flipped, resulting in a change of spin state—often from a singlet to a triplet state. Here, the excited electron is no longer paired to its ground state electron since they no longer have opposite spin. Internal conversion is similar, but instead of dispensing excess energy through a transition of spin state, causing a temporary unpairing of the electrons, the spin state is maintained and the excess energy is given to vibrational modes in the molecule as it falls from its excited state. All of these nonradiative processes result in the shedding of heat to some extent, and when occurring, play a role in TL. Phosphorescence occurs only when a molecule has entered into an abnormal spin state, and then converts back to its original state by the slow emission of a photon. Fluorescence is faster; it occurs when a molecule remains in its usual spin state after excitation and then quickly emits a photon to fall back to the ground state.

Thermal Lensing

Flash Photolysis is a spectroscopic technique developed by Porter and co-workers.[3] Its primary use has been to study fast chemical processes in molecular systems with the use of light. The process entails the use of a flash, or an excitation energy source, to excite a sample. The molecules in the sample absorb the energy, and are promoted to a higher energy state. From here, a second light source, used as a probe, is directed through the

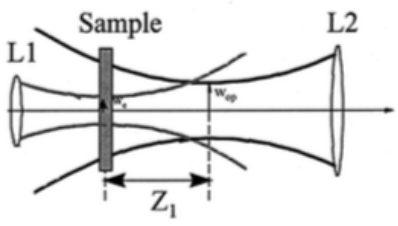

Figure 3: Diagram demonstrating TL effect as probing and excitation beams pass through the sample. L1 is the excitation beam with a smaller beam waist, and L2 is the probing beam with a larger beam waist. This overlap creates the best TL signal. L2 begins diverging at a point beyond the sample and it continues propagating towards the photodiode while L1 dissipates.

sample to monitor what happens to the molecules, as seen in Figure 3.[4] The changes are detected by a photodiode, and displayed on an oscilloscope.

TL is a type of Flash Photolysis. In order for TL to specifically occur in a sample, excited molecules dissolved in a solvent, or in the case of QD, colloidally suspended, need to undergo some sort of nonradiative process, such as vibrational relaxation. When molecules are electronically excited by an excitation source and begin to dispense heat energy into the surrounding solvent by vibrating and colliding with other molecules, the density of the solvent decreases as the solvent molecules begin to move more freely. This heating results in a lowering of the refractive index of the solvent at the point of excitation. Comparatively, the refractive index of the solvent surrounding the incident point is now greater, creating a refractive index gradient in the system. Due to this gradient, light now passes more quickly through the center of the sample than it does on the periphery. This lensing effect ultimately results in the divergence of collimated light (such as a typical laser beam) as it passes directly through the sample (See Figure 4), much like the effect of a double concave lens, but instead of changing the diameter of the medium the probing laser passes through—as a normal lens has a diameter gradient—the refractive index changes.[5] The result is that less light reaches the detector and the signal displayed on the oscilloscope is lessened.

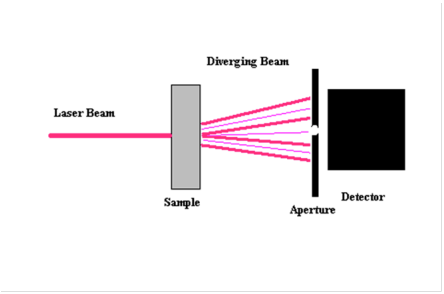

Figure 4: Diagram demonstrating the divergence of the probing laser as it passes through the sample and reaches the photodiode.

Optical Alignment

The TL effect can be simulated and monitored by a mode-mismatched pump-probe optical alignment and, once simulated, the way the TL signal propagates can be analyzed to draw conclusions about the various excited states the molecule experiences and the length of time the excited state transitions are manifested. This optical alignment requires an excitation laser and a probing laser, but it is necessary that the beam waist (the diameter of the laser) of the probing laser be greater than the former so the probing laser will pass directly through the thermal lens, allowing it to experience the full effect of this phenomenon. To this end, the excitation laser is focused onto the center of the cuvette containing the sample, and the probing laser is aligned collinear to it the goal is to establish an ideal overlap of both lasers since the better the overlap within the sample, the better the TL signal. The probing laser is then directed towards a photodiode connected to an oscilloscope, where the electronic signal is generated. As less light reaches the detector due to the generated thermal lens, fewer volts will be generated by the photodiode, and the voltage signal on the oscilloscope will decrease. An example of such a layout is provided in Figure 5.[5]

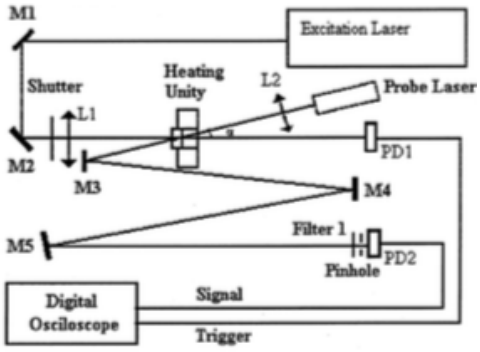

Figure 5: An example of a thermal lensing optical alignment

Experimental Methods

Benzophenone Calibration

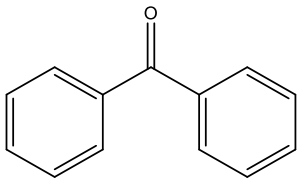

Figure 6. Structure of Benzophenone

Before synthesis of the QD was done, the TL optical alignment was optimized. Since the excited state dynamics of benzophenone is clearly understood, it makes for a useful test molecule for TL; the TL effect is easier to simulate with benzophenone and the signal on the oscilloscope is clearly identifiable. A significant amount of the energy absorbed by benzophenone is lost to nonradiative vibrational modes, allowing for the generation of a strong TL signal. Benzophenone also undergoes intersystem crossing, and is capable of phosphorescence.

A great deal of time was spent at this stage of the experiment setting up the optical bench and tweaking it for a maximum change electrical potential. By varying the conditions of the setup, a signal with the greatest change from baseline readings to the point immediately after excitation could be acquired. Because the TL process occurs at the molecular level in timescales ranging from nano to microseconds, it is challenging to both produce and optimize a signal, so many factors had to be adjusted to accomplish this.

Changes in the experimental conditions included variations in the concentration of benzophenone. Signals were generated using benzophenone dissolved in cyclohexane at concentrations of 0.1, 0.01, 0.005, and 0.001 M. The arrangement of reflective prisms was adjusted to ensure laser alignment and overlap were precise so the signal could be generated; the slightest adjustments in the prisms, including vibrations in the building, could put the lasers out of alignment and result in a loss of signal. The focal lengths of lenses and the alignments of these

lenses were also adjusted. Changes included using either 300 or 500 mm focal lenses for the excitation laser, and on one occasion, using both to attempt to minimize the beam waist of the laser. Cuvette size also made for a notable variable; a smaller cuvette resulted in the generation of more noise on the oscilloscope, potentially due to the increased generation of waves in the sample as the excitation laser was focused and pulsed through the sample. The temperature of the sample solution might have also had an effect on the signal since a change in temperature of the sample solution is vital to the generation of a TL signal; therefore, the TL signal of room temperature and refrigerated samples were compared. It was also found that the older benzophenone samples displayed a decrease in signal, so newer samples were made over the course of this calibration and found to have better signals, initially. Over time, the clarity and displayed change in voltage on the oscilloscope would decrease.

It seemed after this extensive testing that fresh samples of room-temperature benzophenone in cyclohexane at 0.01 M contained in a 1 cm glass cuvette gave the best TL results with the greatest change from baseline to excitation readings. Since the excitation laser discharged a significant amount of electricity that nearby wiring picked up, adequate aluminum shielding of the wiring around the lasers was necessary to minimize noise generated in the oscilloscope. The excitation laser used during the calibration was a SRS NL100 model pulsed N_2 laser (which was later changed during the TL of the QD) and the probing laser was a Melles Griot 10 mW 632.8 nm HeNe laser. A trigger, activated by the slowly pulsed excitation laser passing through a beam splitter, was used to initiate data collection on the Tektronix MDO3024 oscilloscope. The excitation beam passed through a 300 mm focal lens and was directed towards the sample cuvette, collinear to the separate HeNe beam. The excitation beam dissipated but the collimated HeNe beam was directed towards a fast photodiode guarded by a slightly opened

aperture. The oscilloscope picked up the HeNe light that passed through this aperture, providing the TL signal in mV on a μs timescale.

QD Synthesis

The CdSe nanocrystals were synthesized by means of a wet colloidal synthesis. They were synthesized twice, but the UV-Vis and TL data were not formally collected in the original procedure, so the following procedure and data collection originates from the second, optimized synthetic procedure.

To begin, the Se solution was prepared by dissolving 32.6 mg Se powder in 5 mL octadecene with the addition of 0.4 mL trioctylphosphine, heated and stirred in a 10 mL roundbottom flask suspended over a hot plate. 40.3 mg of CdO was then added to a 50 mL roundbottom flask containing a stir bar and 1.9 mL oleic acid was measured out with a syringe and also added to the flask. 30 mL octadecene was added last, and then the flask was placed in a sand bath contained in a variostat-heating element. Stirring and heating was initiated with the aim of achieving a solution temperature of 225 °C. Four test tubes were acquired and labeled from one to four, and a 10 mL mohr pipet and bulb was obtained prior to sampling the solution. An electric thermometer was used to monitor the temperature of the sand bath, and when a temperature of 150 °C was achieved, a glass thermometer was used to periodically check the temperature of the solution. Once the solution arrived at 225 °C, 3.0 mL of the Se solution was added and a timer started. Samples of approximately 5.0 mL were quickly withdrawn from the reaction vessel with the mohr pipet and dispensed into test tubes one, two, three, and four at times 10, 32, 85, and 300 seconds, respectively. The act of withdrawing the solution quenches the reaction as the temperature rapidly drops in the cool glassware, stopping cluster formation

and preserving the nanoparticles in a colloidal suspension. Sample one was yellow, two was orange, three was red, and four was dark red. After the samples reached room temperature, UV-Visible spectroscopy was utilized. Using a PerkinElmer Lambda 465 UV-Vis spectrometer, the longest wavelength peaks in the visible range were recorded. From this point, TL could be performed on each individual sample.

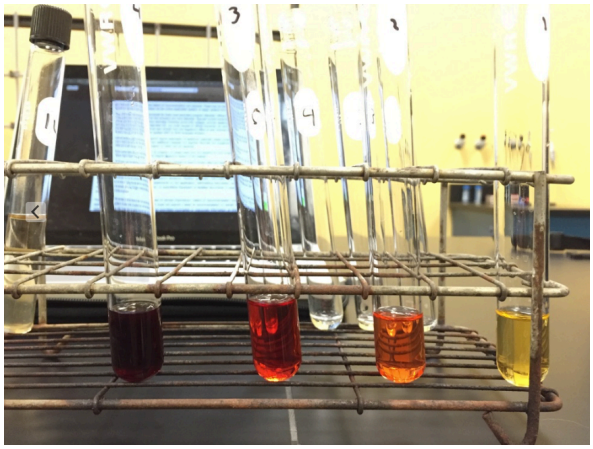

TL Spectroscopy

The greatest hurdle in obtaining a TL signal for the QD was the size of the excitation laser as it hit the sample; it was difficult to focus the beam to a precise point using the SRS NL100 pulsed N_2 laser. As mentioned during the benzophenone calibration, the amount and arrangement of focal lenses was changed in an attempt to focus the excitation laser more tightly. These adjustments proved inadequate. Not until switching to the PTI GL-3300 N_2 pumped laser and the PTI GL-301 Dye laser (N_2/Dye laser) did the beam focus to a precise point on the sample cuvette, allowing for the acquisition of TL data for the QD. Once this obstacle was overcome, TL was performed on each QD sample, immediately after synthesis, in 1 cm glass cuvettes using the same optical alignment as the benzophenone setup, save for the new excitation source. The

N_2/Dye laser was set to 463 nm since all the samples absorbed blue light, as indicated by the UV-Vis spectra.

Dissolved O_2 rapidly absorbs excitation energy by colliding with other excited molecules. For this reason, O_2 is prone to quenching the excited states of other molecules in favor of becoming excited itself, shortening the lifetime of the other molecules excited state transitions. To both observe and minimize this quenching effect of O_2 on the excited states of the QD, each sample was analyzed before and after purging with N_2 gas for a short time. By flowing N_2 into the solution, O_2 gas is slowly purged out of the solution, allowing for data to be collected without O_2 having as much of an effect on the data. Before and after purging, TL data were generated, collected, and then interpreted in the program, Igor Pro 6.37, in order to find the lifetimes of the excited states. The QD were observed to fluoresce when using the SRS NL100 N_2 laser—since it operates in the UV range, invisible to the eye—as the samples emitted blue light after every excitation pulse. However, the subsequent data analysis is devoid of adequate and clear information regarding this radiative process.

Data Analysis

Equation 1, formulated by Yu et al., is used for determining the radius (a) of the nanoclusters using the wavelength (λ) of the longest absorption maximum, as determined by UV-Visible spectroscopy.[6]

$$a = 0.8061 * 10^{-9}\lambda^4 - 1.3288 * 10^{-6}\lambda^3 + 0.8121 * 10^{-3}\lambda^2 - 0.2139\lambda + 20.79 \qquad (1)$$

The following exponential fit equation, equation 2, is used for graphical analysis in Igor Pro 6.37. By integrating the first-order kinetics expression, which represents the kinetics of excited state processes, it can be determined that excited energy states decay exponentially. This relationship allows the use of the exponential fit equation on Igor to analyze the TL data. This expression contains the term, τ, which represents the lifetimes of the excited state transitions and can be solved for from this equation.

$$y_0 + A * \exp\left(-\frac{1}{\tau} * x\right) \qquad (2)$$

Equation 3 solves for the fraction thermal load (φ), which is representative of the fraction of energy given to nonradiative processes. It contrasts the fluorescence quantum efficiency, which is the fraction of energy given to radiative processes in the system. 1 represents the total quantum efficiency, and effectively represents 100% energy usage in the molecule, while η is the fluorescence quantum efficiency, λ_e is the excitation beam wavelength, and λ_{em} is the fluorescence emission wavelength. This equation was obtained from Pilla et al.[7]

$$\varphi = 1 - \eta \frac{\lambda_e}{\lambda_{em}} \qquad (3)$$

Results

Figure 4 is the spectrum generated by the UV-Vis spectrometer. The longest wavelength of absorbed light in the visible range was determined for samples 1 through 4 in this spectrum.

Figure 4. UV-Vis Spectrum

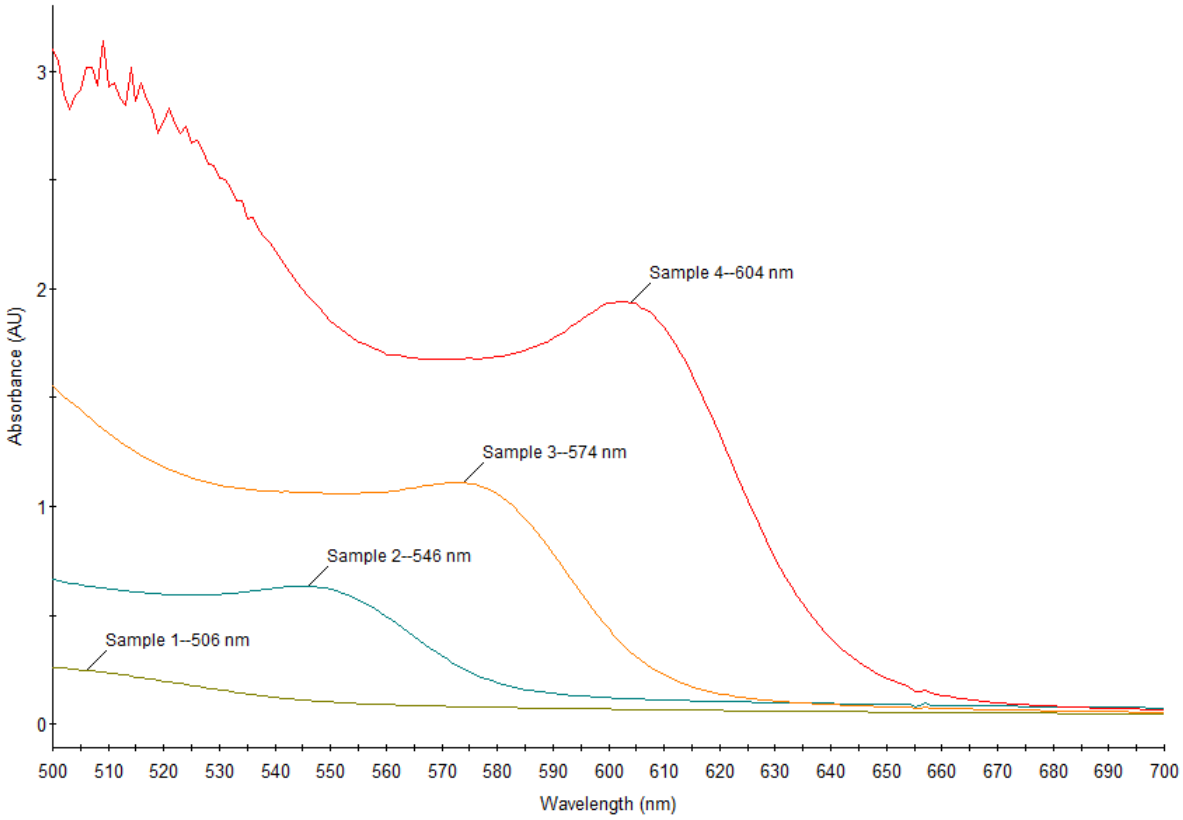

Using equation 1 and the longest λ peak from Figure 4, the radius of each QD was calculated and recorded in Table 1.

Table 1. Particle Size

	Longest λ (nm)	Radius (nm)
Sample 1	506	1.17
Sample 2	546	1.45
Sample 3	574	1.78
Sample 4	604	2.34

Figures 6 through 13 show the raw TL data generated in Excel. The baseline before t=0 records the amount of light reaching the detector before the simulation of the thermal lens, and the signal generated after t=0 shows the decreased amount of light reaching the detector after excitation.

Figure 5. TL Signal for Sample 1 Before Purging with N_2

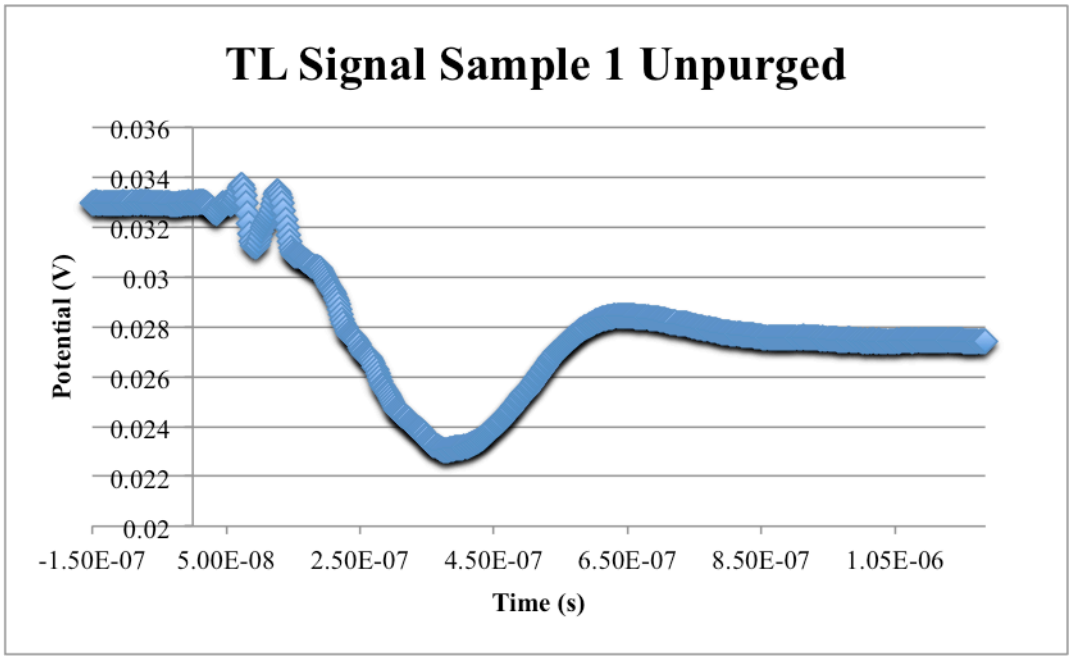

Figure 6. TL Signal for Sample 1 After Purging with N_2

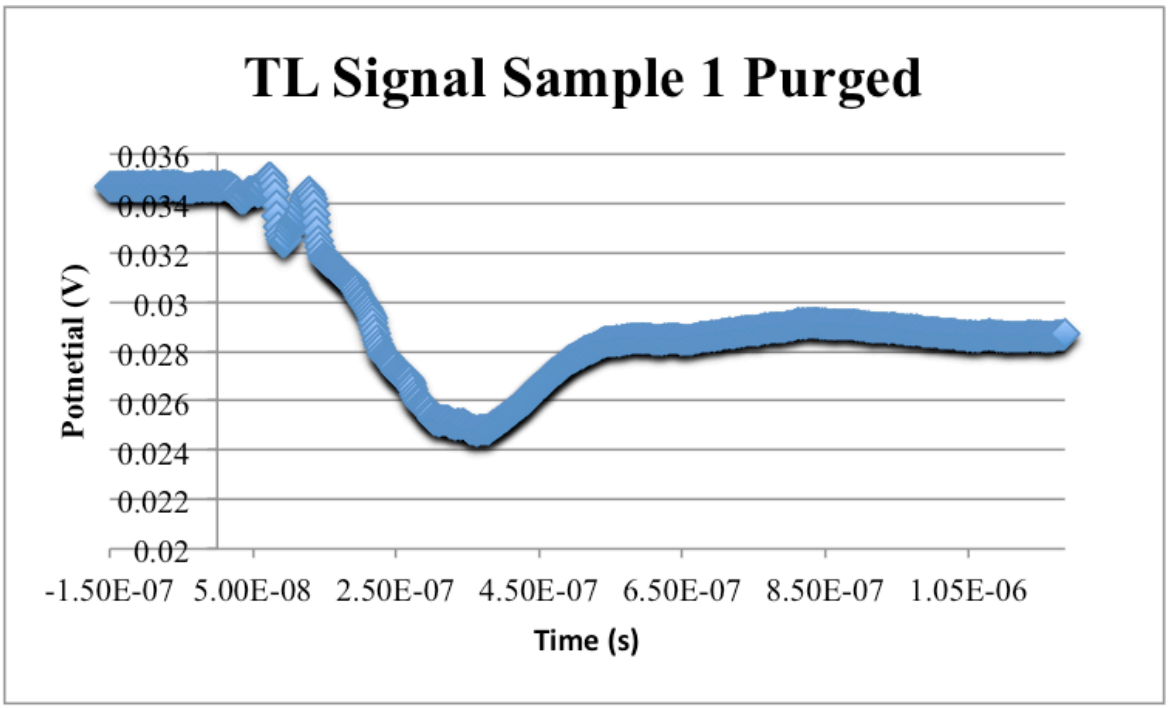

Figure 7. TL Signal for Sample 2 Before Purging with N_2

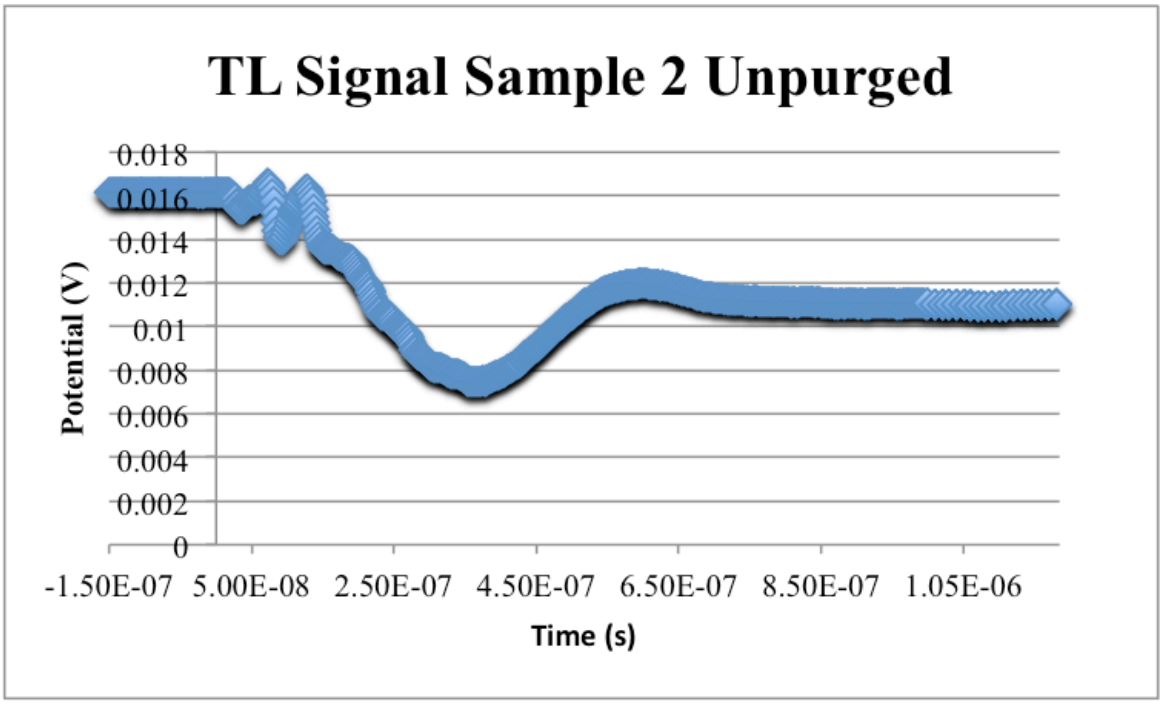

Figure 8. TL Signal for Sample 2 After Purging with N_2

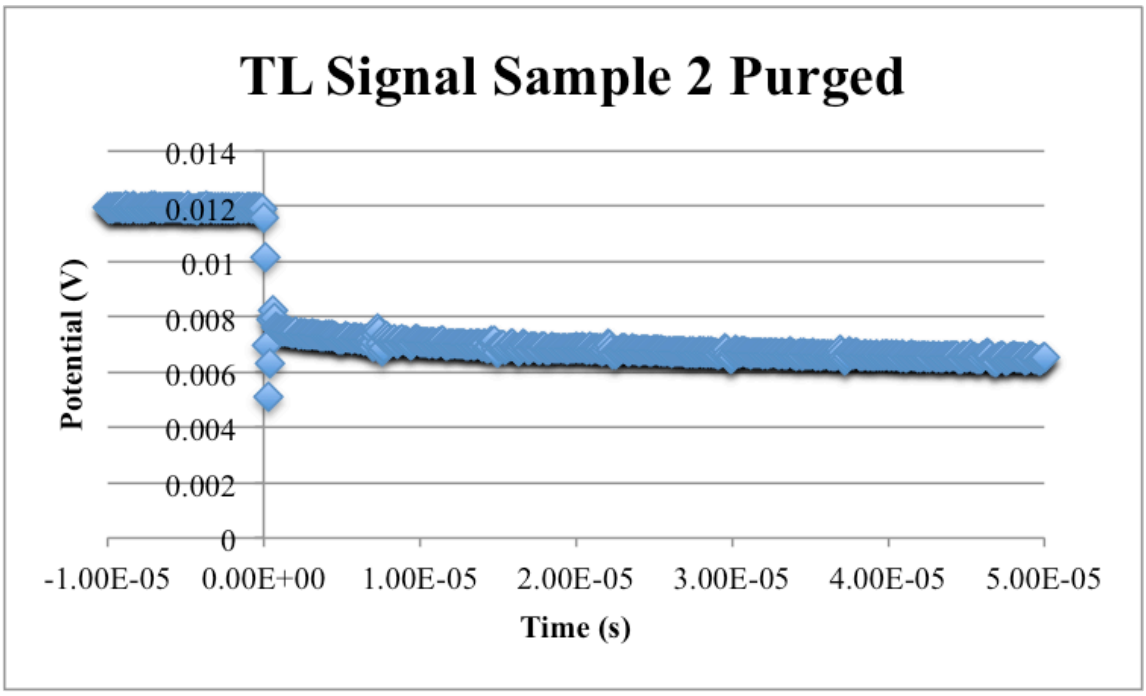

Figure 9. TL Signal for Sample 3 Before Purging with N_2

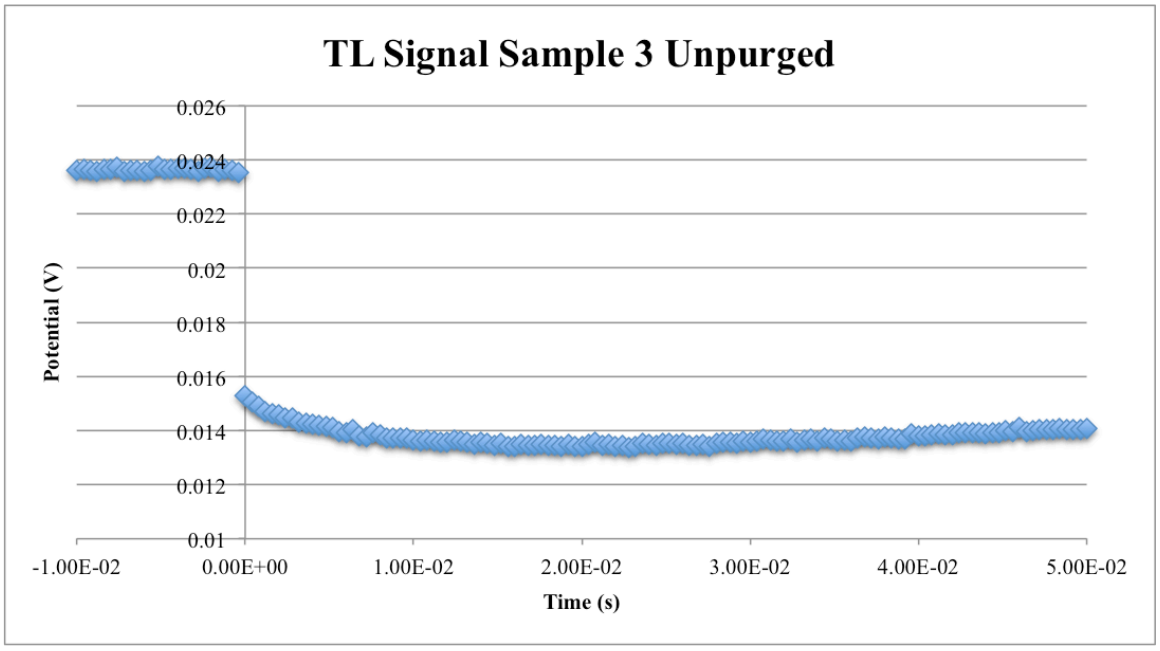

Figure 10. TL Signal for Sample 3 After Purging with N_2

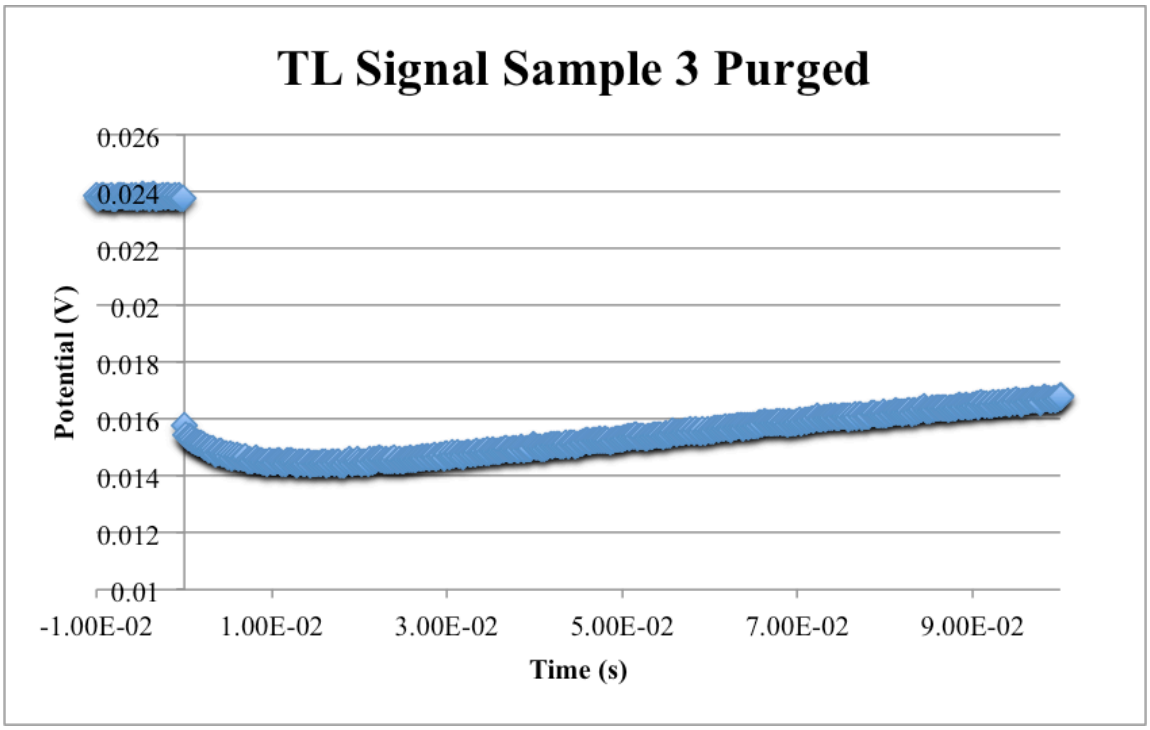

Figure 11. TL Signal for Sample 4 Before Purging with N_2

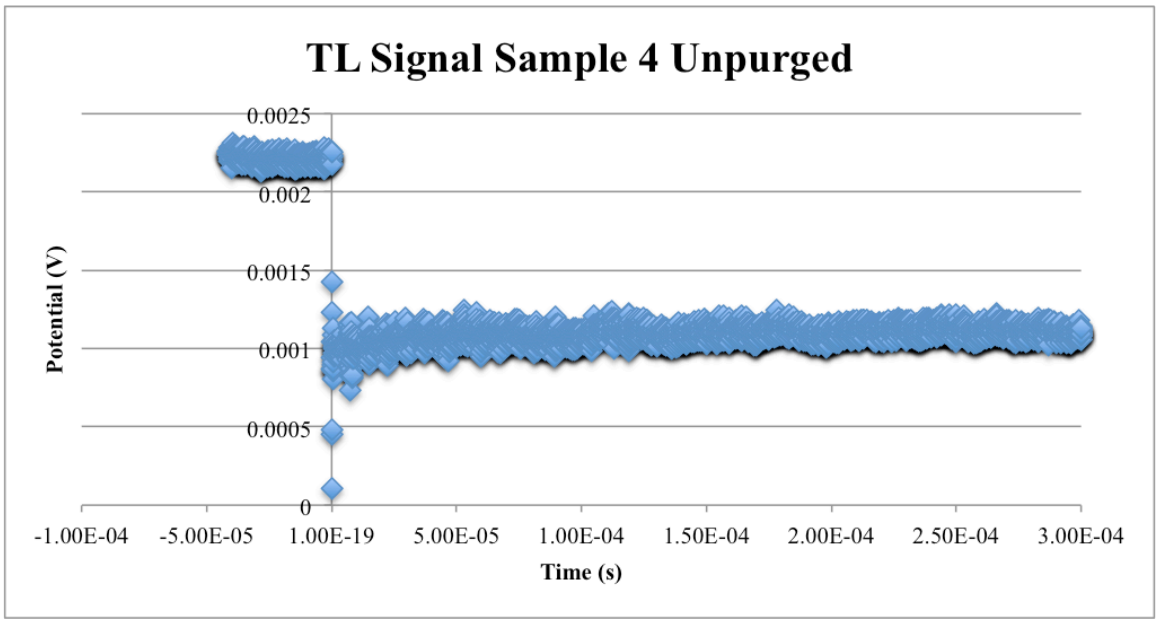

Figure 12. TL Signal for Sample 4 After Purging with N_2

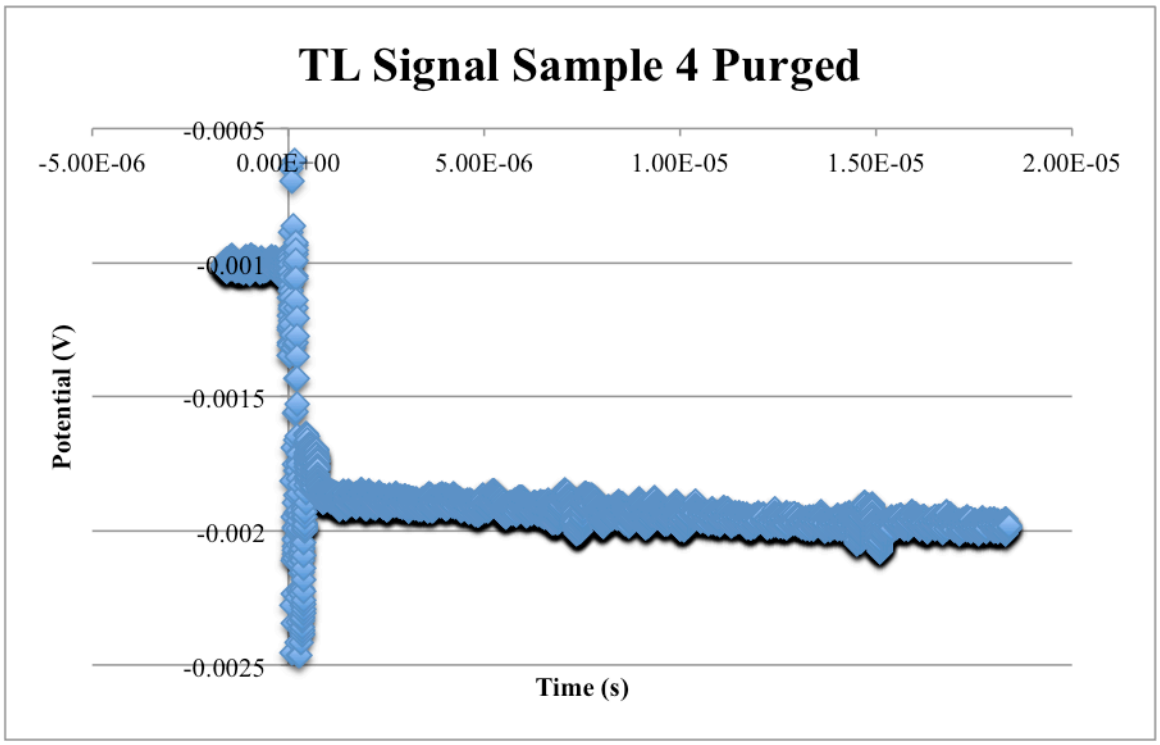

The raw TL data was uploaded into Igor and used to generate figures 13 through 17. Each of these graphs compares the samples before and after purging with N_2, and shows examples of an exponential fit used to analyze the data.

Figure 13. Igor Analysis Sample 1

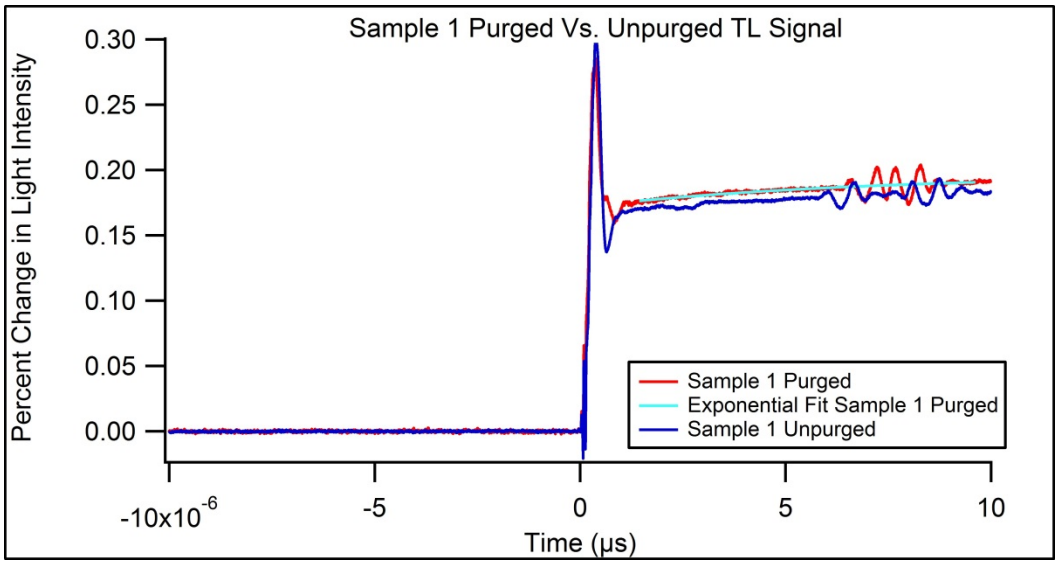

Figure 14. Igor Analysis Sample 2

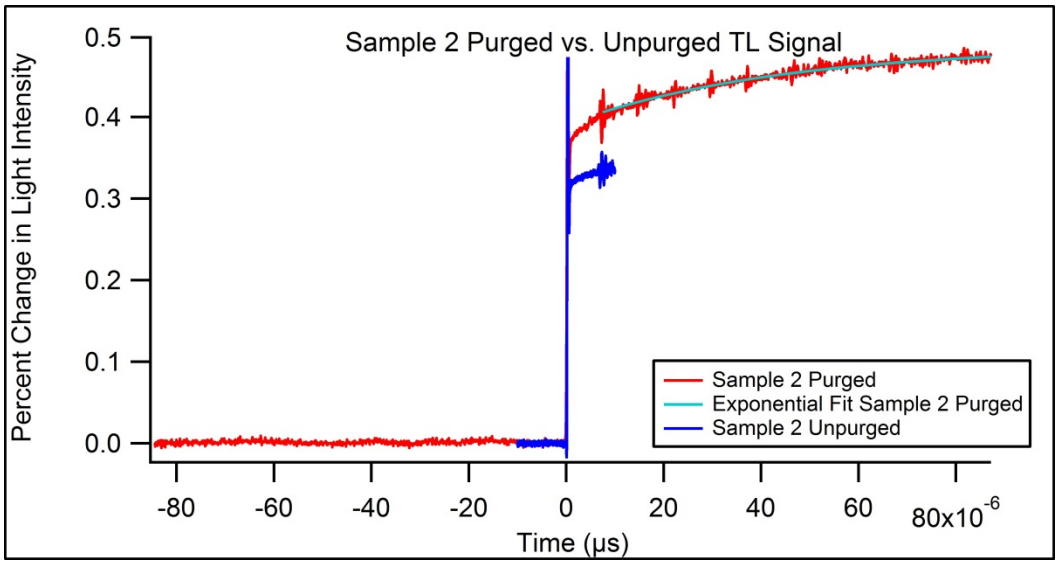

Figure 15. Igor Analysis Sample 3

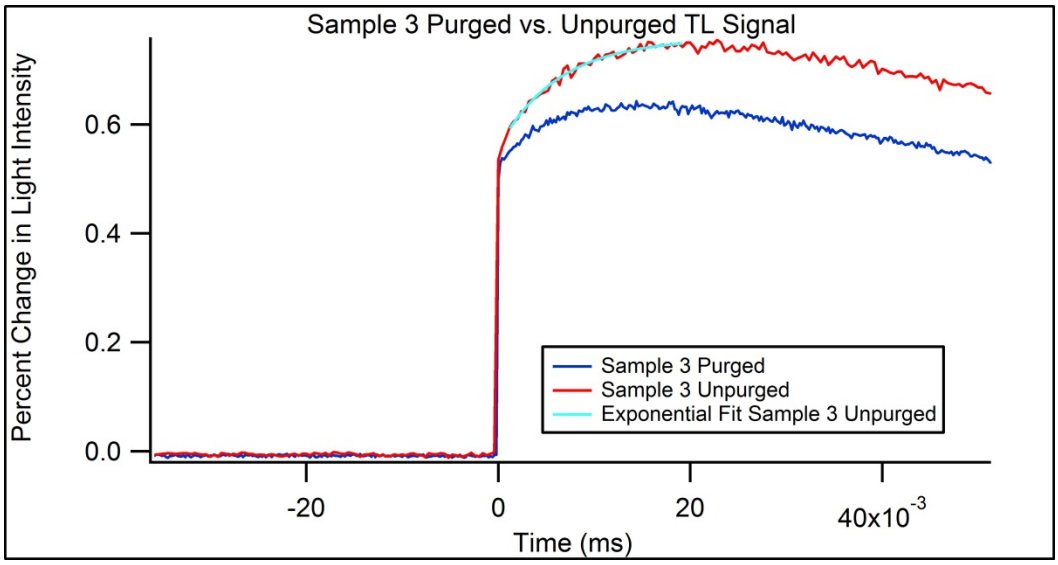

Figure 16. Igor Analysis Sample 4

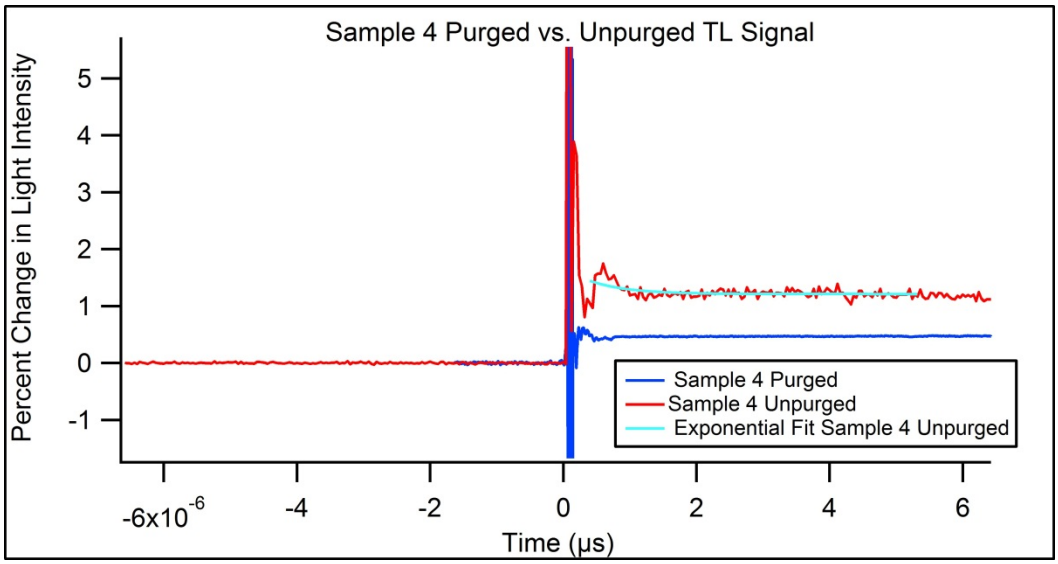

Using Igor, the rate constant for each TL sample was determined after converting the raw TL data into figures 14 through 17 and fitting equation 2 to the data. Taking the inverse of the

rate constant term, $\frac{1}{\tau}$, from equation 2 allows τ to be found; this lifetime value was recorded in Table 2.

Table 2. Lifetimes of Excited States

	Rate Constant (μs^{-1})	Lifetime τ (μs)
Sample 1 Unpurged	0.1393 +/- 0.009890	7.178 +/- 0.5096
Sample 1 Purged	0.1737 +/- 0.01340	5.757 +/- 0.4441
Sample 2 Unpurged	0.7256 +/- 0.01470	1.378 +/- 0.02792
Sample 2 Purged	0.02312 +/- 0.0001540	43.25 +/- 0.2881
Sample 3 Unpurged	0.0001465 +/- 0.00002200	6827 +/- 1025
Sample 3 Purged	0.0002335 +/- 0.00001800	4282 +/- 330.1
Sample 4 Unpurged	0.03089 +/- 0.005220	32.37 +/- 5.471
Sample 4 Purged	9.545 +/- 0.3330	0.1047 +/- 0.003653

Figure 17 shows the relationship between the lifetimes of the excited state transitions and the radius of each QD. According to this graph, there is no discernable relationship between the two. Sample 3 was excluded from this data because its lifetime is drastically longer than the other samples, skewing the data even further.

Figure 17. Graph of Radii Vs. Lifetimes of the Excited States

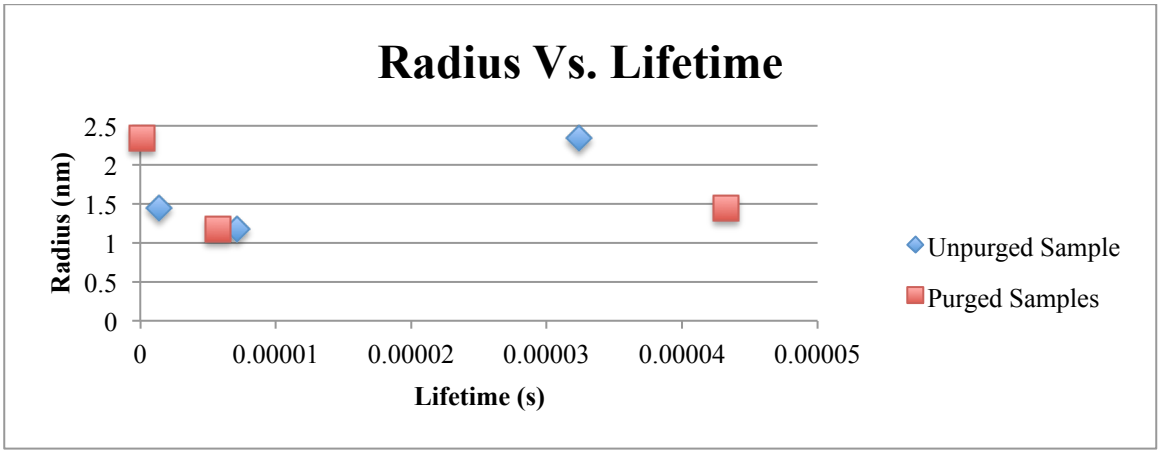

Discussion

As determined from the UV-Vis absorption spectra, each consecutive sample of QD taken exhibited an increase in particle size, indicating a successful synthesis. Each sample also provided a TL signal, which clearly indicates these molecules are excited by blue light and undergo vibrational relaxation to dispense some of this energy.

However, according to the data displayed by Figure 17, no apparent relationship seems to exist between size of the particle, and the lifetime of the excited state analyzed from TL. There are many unclear differences between the purged and unpurged samples, sizes of particles, and lifetimes. The largest purged sample, sample 4, had the shortest lifetime while sample 2, purged, had the longest. There seems to be no clear reason for this observation. Sample 3 was entirely excluded from this data set because the TL signal did not have enough data point density at the point of excitation to analyze it clearly and conclusively in Igor. It became an outlier for this comparison, though it does exhibit some sort of excited state phenomenon on a broader scale, boasting the longest lifetime of the sample set.

Sample 3 had a lifetime on a ms scale while all the other samples vacillated around a μs scale, as seen in Table 2. A ms timescale, if accurately representing an excited state process and not simply the recovery of the system back to temperature equilibrium, would suggest intersystem crossing, as it is the slowest of the nonradiative processes. Since sample 3 is the only sample data were acquired on such a long timescale, it would be worth investigating the other samples to see if they have processes that last for as long. If QD undergo intersystem crossing, more testing would need to be done to determine how and when the electrons return to their original spin state.

Another factor perhaps affecting the clarity of these data and inhibiting conclusions from being drawn is the method by which purging the cuvettes with N_2 were done; the samples were not purged at strictly the same time intervals. Sample 4 was purged significantly longer than the others, which is perhaps why it had a decidedly shorter lifetime. Though, if O_2 quenches and shortens excited states, this is the opposite conclusion than would have been expected—the purged sample should have a significantly longer lifetime than the unpurged. Perhaps the excited state of O_2 can occasionally delay in generation, from which point it adds its lifetime to the thermal lensing signal and artificially lengthening the lifetime under investigation for the unpurged sample. To get a more accurate depiction of the involvement of O_2 in the QD excited state processes, a more thorough means of purging the samples would have to be formulated.

On the other hand, perhaps there is some other distinctly different process sample 4 is experiencing. Sample 4 absorbs red light, as shown by its absorption spectrum; this means the probing laser was not only probing the sample, but it was involved in its excited state processes. The signal is significantly weaker for this reason, and might give rise to a different kind of excited state process than the other samples. Based on the graphical analysis, less light from the HeNe laser reaches the detector over a short timeframe rather then more, like the other samples. This might indicate Transient Absorption, a process necessitating the excitation of a molecule to a higher electronic state, from which point it begins to absorb a different wavelength of light—in this case, more effectively absorbing red light. This means for a time after excitation, the molecules are absorbing more light and allowing less of it to reach the photodiode. To verify this would require further testing both with the current optical alignment, and with a laser in the far red to infrared to ensure absorption by the sample does not occur.

The fluorescence quantum efficiency could not be determined since fluorescent emission was not effectively recorded. As previously indicated, these samples of QD do fluoresce, but the data from a fluorometer could not be acquired in time to verify how efficiently these samples use excitation energy. A simple emission spectrum would need to be generated for each sample in order to determine this value.

Fluorescence lifetimes are incredibly fast, occurring in nanosecond timescales. Since fluorescence occurs almost immediately after excitation, the limitations of the TL technique become more apparent. Without a small enough beam size and a quick enough photodetector, the fluorescence signal is lost in the overall signal as the TL signal itself can take hundreds of nanoseconds to develop, and by then, the part of the signal that could be attributed to fluorescence has long since dissipated. This error can contribute to errors in the calculated lifetime of the excited state, since the fluorescence is not accurately being represented.

The fraction thermal load could not be determined since the fluorescence quantum efficiency was not determined. Without this data, equation 3 could not be used to determine the energy lost due to nonradiative processes.

Regarding why analyses of these QD solutions had to be done immediately after synthesis—the QD did not appear to remain stable over an extended period of time. From the first QD synthesis performed, it was noted the solutions changed and dulled in color after freezing. Freezing was done with the intent of preserving the QD by immobilizing them in the colloidal suspension. However, this did not prevent aggregation of the particles into visibly perceived clusters and the color dulling was also a perceived result of their storage. During the second trial, the TL and UV-Vis analyses were performed within the day of their synthesis, and all the acquired data are a result of this procedure. However, over time, these solutions also

aggregated into visible clusters, with one notable difference—the colors of the solutions remained as vivid and clear as they initially appeared. For further qualitative comparison, the residual reaction mixture was left in the dark for a few weeks while the acquired sample were left in contact with more sunlight for the same period of time. It appeared the samples aggregated larger crystals than the leftover reaction mixture. This would seem to suggest the QD could maintain some sensitivity to temperature and undergo some other slow process in the presence of light that results in the aggregation of nanoclusters.

With this analysis of the data in mind, there are more complicated synthetic methods and processes regarding these QD than are discussed within the scope of this work. There is a great deal of frontier research too expensive for the facilities of Bellarmine University to currently investigate. CdSe is still being studied in this kind of research, but with a handful of distinct improvements. Core-shell type QD are garnering interest in research, solely because these molecules have improved quantum efficiency; the difference in structure is attributed to the addition of another layer of nanoparticles surrounding the core, which creates a type of allosteric effect on the particle to improve its capabilities.[7] An example molecule of this kind would be CdSe/ZnS, which is a QD with a CdSe core and a ZnS shell. Some research also looks into the effect embedding these molecules into matrices have on their quantum efficiency—even solvent effects are being investigated, as we see in the work of Pilla and co-workers. There is a broad realm opening up in research for improving the effectiveness and applications of these molecules as new ideas are being coupled with QD.

Conclusion

Four different solutions of quantum dots were synthesized, collected, and analyzed. UV-Visible spectroscopy allowed the size of these particles to be determined, and TL provided some insight into how these molecules use energy when they enter an excited state. They certainly fluoresce and vibrationally relax, to no surprise, but the nature of their overall quantum yield could not be determined. However, TL did allow the discovery of the lifetimes of currently unknown excited states. Each lifetime varied by some degree based on particle size and dissolved O_2 concentrations in the octadecene solvent. A more systematic approach must be made in the future regarding purging the O_2 and collecting the TL in precisely the same timeframe, studying both the early stages of the TL signal, and the latter stages to allow a more concrete determination of the processes these molecules undergo, and the relationship between those processes and the size of each particle. Fluorescence data would also be useful in determining the quantum efficiency of these molecules.

Closing Statement

Over the course of this project, I learned how a great deal about the ins and outs of putting together and executing a large-scale piece of work. I learned how to sift through journals and articles to find information pertinent to the project I needed to piece together. Through this process I better developed a better sense of how to synthesize research, experimentation, and analysis into a cohesive body of work that is both comprehensive and relatively succinct. Though this project did not yield effective results, teaching the all too common motif that research will often fail, it does lay the foundation for further studies and experimentation in order to gain more conclusive evidence and insight into how these molecules, QD, utilize energy, and subsequently,

how we may use them to ourselves better utilize energy. Writing this thesis has been invaluable to me as someone who will be entering the professional scientific field and will likely write reports, papers, or articles similar to this on a regular basis. Familiarizing myself with this kind of work will better prepare me for the work I expect to see in the future, and now I find I am not nearly as daunted by that thought.

References

[1] Coe-Sullivan, Seth. "Are Quantum Dots on the Brink of Their Big Break?" *Photonics.com*. Photonics Spectra, May 2007. Web. 20 Apr. 2016.

[2] Prescher, Jens. "Establishment and Optimization of Super-Resolution Fluorescence Microscopy for Multi-Colour Studies of Biological Systems." (1984): n. pag. *Http://www.cup.uni-muenchen.de/pc/lamb/pdf/Jens_Prescher_Masterarbeit.pdf*. Ludwig-Maximilians-Universität München. Web.

[3] Porter, G. *Proc. R. Soc. London Ser. A* **1950**, 200, 284-299

[4] Holt, Patrick. "Ch. 9 Flash Photolysis of Benzophenone." Ed. Richard W. Schwenz. *Physical Chemistry: Developing a Dynamic Curriculum*. Ed. Robert J. Moore. Washington, D.C.: American Chemical Society, 1993. 151-65. Print.

[5] Lima, S.m., J.a. Sampaio, T. Catunda, A.c. Bento, L.c.m. Miranda, and M.l. Baesso. "Mode-mismatched Thermal Lens Spectrometry for Thermo-optical Properties Measurement in Optical Glasses: A Review." *Journal of Non-Crystalline Solids* 273.1-3 (2000): 215-27. Web.

[6] Yu. W.; Qu, L.; Peng, X. *Chem Mater.* **2003,** 15, 2845.

[7] Pilla, Viviane; Leandro P. Alves; Egberto Munin; and Marcos T.t. Pacheco. "Radiative Quantum Efficiency of CdSe/ZnS Quantum Dots Suspended in Different Solvents." *Optics Communications* 280.1 (2007): 225-29. Web.

[8] Boatman, E. M.; Lisensky, G. C.; Nordell, K. J. *J. Chem. Ed.* **2005**, 82, 1697—1699.